View metadata, citation and similar papers at core.ac.uk
brought to you by CORE
provided by Repositorio da Producao Cientifica e Intelectual da Unicamp

PHYSICAL REVIEW A **77**, 012717 (2008)

Polarization effects on electronic excitation of molecules by low-energy electron impact: Study on e^--furan scattering

Romarly F. da Costa,[1] Márcio H. F. Bettega,[2] and Marco A. P. Lima[1]
[1]*Instituto de Física Gleb Wataghin, Universidade Estadual de Campinas, Caixa Postal 6165, 13083-970, Campinas, SP, Brazil*
[2]*Departamento de Física, Universidade Federal do Paraná, Caixa Postal 19044, 81531-990, Curitiba, Paraná, Brazil*
(Received 31 August 2007; published 23 January 2008)

The Schwinger multichannel method is applied to study the influence of polarization effects on the electronic excitation of the furan molecule by low-energy electron impact. We discuss the importance of inclusion of these effects through the comparison of theoretical results for the electronic excitation of the $^3B_2$ state of furan obtained with and without the proper treatment of the polarization of the target. The electron-furan scattering presents two prominent shape resonances in the $^2A_2$ and $^2B_1$ symmetries at around the electronic excitation threshold of the $^3B_2$ state (3.7 eV). At this low-energy, the inclusion of polarization effects in the calculation moves to lower energies the resonances positions obtained either in the close-coupling or in the static-exchange level of approximation. This phenomenon strongly influences the electronic excitation process. The present results show that a simple close-coupling calculation cannot be applied for molecular systems with low-energy electronic excitation thresholds around misplaced resonances.

DOI: 10.1103/PhysRevA.77.012717 PACS number(s): 34.80.Gs, 34.80.Bm

I. INTRODUCTION

In a set of recent publications, Sanche and co-workers have pointed out that single- and double-strand breaks in DNA induced by secondary low-energy electrons (below 20 eV) play a key role for the understanding of the damage effects of ionizing radiation in living cells and tissues [1]. Such discovery has stimulated a strong interest on studies concerning the scattering of slow electrons by biological molecules.

The effort undertaken by theoretical and experimental groups in order to provide a deeper insight into the mechanisms underpinning the radiation damage to DNA includes both direct processes (ionization, electronic, rotational and vibrational excitations) as well as indirect processes mediated by resonances (dissociation and dissociative electron attachment). These studies can be divided in two research lines, i.e., (i) those involving nucleic acid bases or its fragments [2–6] and (ii) those involving other molecules carrying structural or functional properties similar to those of small parts of DNA [6–10].

An interesting feature that most of these molecules have in common is the presence of a first excited triplet state lying at around 3 to 4 eV [11]. It is well known that at this range of electron impact energies the inclusion of polarization effects is very important for an accurate description of the scattering process, especially with respect to the location of resonances positions. To better understand the influence of these effects on such a low electronic excitation process we carried out a series of calculations for the transition out of ground state to the $^3B_2$ state of the furan molecule. We have chosen this molecule since it represents a simpler but similar system to the tetrahydrofuran molecule (a sugarlike component of the backbone of the DNA) and also because it presents two prominent shape resonances around the $^3B_2$ excitation threshold [10,12–14]. To carry out this study we have used the Schwinger multichannel method (SMC) with pseudopotentials (SMCPP).

II. THEORY

The SMC and SMCPP methods were discussed in detail elsewhere [15,16]. Here we only give an outline of the method in order to highlight the most important aspects of its theoretical formulation. In the SMC method the scattering amplitude (in the body frame) is given by

$$f(\vec{k}_f,\vec{k}_i) = -\frac{1}{2\pi}\sum_{m,n}\langle S_{\vec{k}_i}|V|\chi_m\rangle(d^{-1})_{mn}\langle\chi_n|V|S_{\vec{k}_f}\rangle, \qquad (1)$$

where the χ_m's are $(N+1)$-electron Slater determinants, constructed from products of target states, obtained by single-configuration interaction (SCI) with one-particle wave functions, keeping only overall doublet states, if the target is a closed shell system [17]. The d_{mn} matrix elements are given by

$$d_{mn} = \langle\chi_m|A^{(+)}|\chi_n\rangle \qquad (2)$$

and the $A^{(+)}$ operator can be written as

$$A^{(+)} = \frac{1}{2}(PV+VP) - VG_P^{(+)}V + \frac{\hat{H}}{N+1} - \frac{1}{2}(\hat{H}P + P\hat{H}). \qquad (3)$$

In the above equations $S_{\vec{k}_{i(f)}}$ is an eigenstate of the unperturbed Hamiltonian H_o, given by the product of a target state and a plane wave with momentum $\vec{k}_{i(f)}$; V is the interaction potential between the incident electron and the target; $\hat{H} \equiv E-H$ is the total energy of the collision minus the full Hamiltonian of the system, with $H=H_o+V$; P is a projection operator onto the open-channel space and $G_P^{(+)}$ is the free-particle Green's function projected on the P space. Our calculations were done with pseudopotentials of Ref. [18] in order to represent the inner electrons close to the nuclei, as described in Ref. [16]. The Cartesian Gaussian functions used in the present calculations are the same used in Ref. [10] and were generated according to Ref. [19].

The analysis for numerical stability of the present calculations is performed through a check procedure developed by

 ©2008 The American Physical Society

Chaudhuri and co-workers to investigate the origin of unphysical resonances appearing in positron-N_2 calculations [20]. Adapted to the case of electron-molecule scattering [17], the analysis begins with the diagonalization of the matrix elements of the $\tilde{V}$ operator

$$\tilde{V} \equiv \frac{1}{2}(PV + VP) + \frac{\bar{H}}{N+1} - \frac{1}{2}(\bar{H}P + P\bar{H}), \tag{4}$$

where V, P have already been defined and $\bar{H}=\hat{H}$, calculated at a fixed energy, following Refs. [17,20]. A next step consists in the identification and elimination of the configurations weakly coupled by this average potential, that is, the eigenvectors associated to the eigenvalues near to zero of the equation $\tilde{V}|\tilde{\chi}_m\rangle = v_m|\tilde{\chi}_m\rangle$. The $\tilde{\chi}_m$'s are then used as a new $(N+1)$-electron basis functions.

III. COMPUTATIONAL DETAILS

We present in this paper the cross sections obtained within the minimal orbital basis for single configuration interactions (MOB-SCI) approach [17] out of the b_1 and a_2 occupied orbitals. The idea is based on the fact that an excited state constructed with an improved virtual orbital (IVO) [21], and calculated for a specific hole orbital, is equivalent to a complete SCI calculation out of the same hole orbital that generated the IVO. This assumption allows the construction of a pair of particle orbitals that provides a minimal configuration basis set fully equivalent to the complete SCI calculation of chosen singlet and triplet states. In practice, the implementation of the MOB-SCI strategy was undertaken as follows. Aiming the state originated by $b_1 \rightarrow a_2$ transition, we have first constructed a subspace composed by two orbitals (two a_2 types), for singlet and triplet IVO's out of b_1 orbital. By running a full SCI calculation we have found that the transition $a_2 \rightarrow b_1$ was strongly coupled to the $b_1 \rightarrow a_2$ one. So, we have also constructed a subspace composed by two orbitals (two b_1 types), for singlet and triplet IVO's out of a_2 orbital. Our active space for the SCI calculation was therefore composed by two holes (b_1 and a_2) and four particles (two IVO's of b_1 and two of a_2 symmetry). These four IVO's are then orthogonalized among themselves, and all remaining orbitals are made orthogonal to them, through the usual Gram-Schmidt procedure (note that the IVO's are, by construction, orthogonal to the ground state orbitals). This strategy allows a small expansion set of single-excitation configurations, and gives rise to two 4×4 matrices for the B_2 symmetry, one for the triplet and another for the singlet Hamiltonians. The diagonalization of these matrices results in a set of triplet and singlet states similar to the complete SCI calculation. It is not totally equivalent because we have used IVO's from two occupied orbitals. This procedure furnishes an electronic excitation energy of 3.7 eV for the $^3B_2$ state, to be compared with 3.3 eV, obtained using a complete SCI calculation, and with 4.4 eV, obtained with the symmetry-adapted cluster configuration-interaction method [22]. Our threshold is in good agreement with the energy loss spectra experimental value of around 4.0 eV [23,24]. The compact vector space obtained by means of the MOB-SCI technique is composed by the physical excited singlet and triplet states along with a minimum set of pseudostates, which slightly polarize the target. By freezing the occupied orbitals and the active particle orbitals described above, we have diagonalized the cation Hamiltonian (two electrons subtracted from the a_2 occupied orbital) and generated modified virtual orbitals (MVO's) [25] from the remaining virtual orbitals. MVO's are known to be efficient in the composition of the configuration space to account for polarization effects [26].

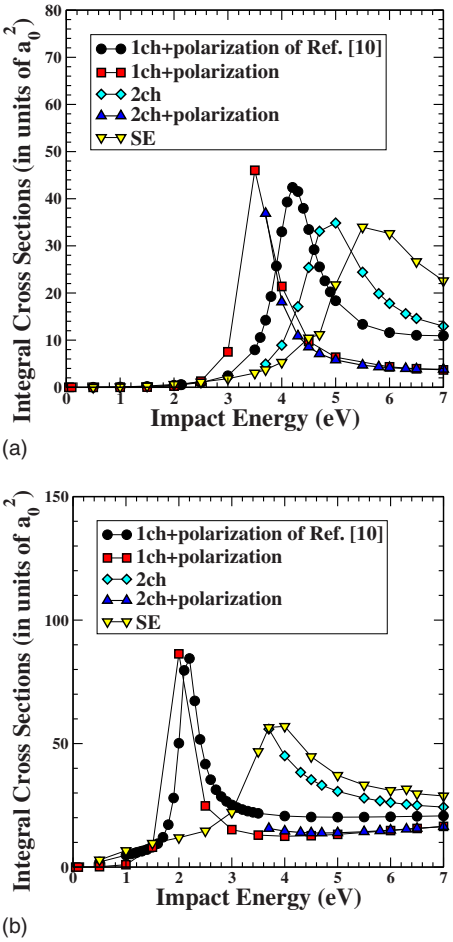

FIG. 1. (Color online) Integral cross sections for the $^1A_1 \rightarrow {}^1A_1$ electronic transition (elastic) of the furan molecule: (a) $^2A_2$ symmetry and (b) $^2B_1$ symmetry. In the legend box: "1ch" means that only the elastic channel is open and "2ch" means that elastic ($^1A_1$) and inelastic ($^3B_2$) channels are open. "SE" means 1ch-static-exchange cross sections.

IV. RESULTS AND DISCUSSION

Figures 1(a) and 1(b) show our elastic results for the resonant symmetries of e^--furan scattering. The yellow down-triangles are obtained at the static-exchange (SE) level of approximation, i.e., in which the molecular state is kept frozen during the collision process, except for the exchange interaction. The resonance in the $^2A_2$ symmetry appears at 5.8 eV while in the $^2B_1$ symmetry it shows at around 4.0 eV. The black circles are results of Ref. [10], obtained with the present method (and basis set) at the static-exchange-plus-

polarization level of approximation. In these calculations the resonant states appear, as expected, at lower energies, located at 4.2 eV for the $^2A_2$ and at 2.2 eV for the $^2B_1$ symmetry. In that presentation the authors followed the rule of taking hole and particle orbitals with the same space symmetry to construct the configuration space and used only one MVO of the resonant symmetry as scattering orbital, thus avoiding over correlation. The red squares are obtained relaxing this condition, that is, taking all single excitations from the hole (occupied) orbitals to all MVO's having negative eigenvalues and those with positive eigenvalues smaller than 10 eV (particle orbitals), and using only the particle orbitals as scattering orbitals. This procedure makes the resonances positions move to even lower energies, 3.4 eV and 2.0 eV, for $^2A_2$ and $^2B_1$ symmetries, respectively, coming in closer agreement with the experimental values of 3.15 eV for $^2A_2$, and of 1.73 eV for $^2B_1$ [12]. The cyan losangles show the elastic cross section obtained with the 2-channel level of approximation (only the small active space generated by the MOB-SCI approach described above polarizes the target). The resonances positions seem to be much closer to those obtained at the SE approximation, i.e., at around 5.0 eV and slightly below 4.0 eV, for $^2A_2$ and $^2B_1$ symmetries, respectively. Finally the blue up-triangles are results obtained with 2-channel coupling (ground $^1A_1$ and excited $^3B_2$ states) using the same level of polarization as used in the red square calculations. It can be noted that the channel coupling (opening the $^3B_2$ state) causes a small change in the elastic cross section compared to the case where this state appears (fictitiously) as closed. Figures 1(a) and 1(b) show that the resonances positions strongly depend on the level of polarization effects considered in the calculation. Figures 2(a) and 2(b) show our electronic inelastic $^1A_1 \rightarrow {}^3B_2$ cross sections for the resonant symmetries of e^--furan scattering. The cyan losangles show the inelastic cross section obtained with the 2-channel level of approximation. The blue up-triangles are results obtained by adding a large set of configurations for polarization effects to the 2-channel calculation. The corresponding elastic cross sections of these inelastic cross sections are shown with the same symbols in Figs. 1(a) and 1(b). The resonance in the close-coupling calculation of the $^2A_2$ symmetry for the elastic channel [cyan losangles of Fig. 1(a)] also decays to the inelastic channel [cyan losangles of Fig. 2(a)]. As the resonance moves below threshold by inclusion of polarization effects [blue up-triangles of Fig. 1(a)] the inelastic cross section diminishes substantially [blue up-triangles of Fig. 2(a)]. Similar situation is seen in the $^2B_1$ symmetry, except that now the resonance in the close-coupling calculation appears near threshold for the elastic channel [cyan losangles of Fig. 1(b)] and shows a strong threshold behavior in the inelastic channel [cyan losangles of Fig. 2(b)]. Again, as the resonance position moves below threshold by inclusion of polarization effects [blue up-triangles of Fig. 1(b)] the inelastic cross section diminishes substantially [blue up-triangles of Fig. 2(b)]. The elastic and inelastic channels can be regarded as two slits of electronic interference. The scattering potential defines the importance of each slit and the presence of a resonance strongly influences the intensities of the exit channels.

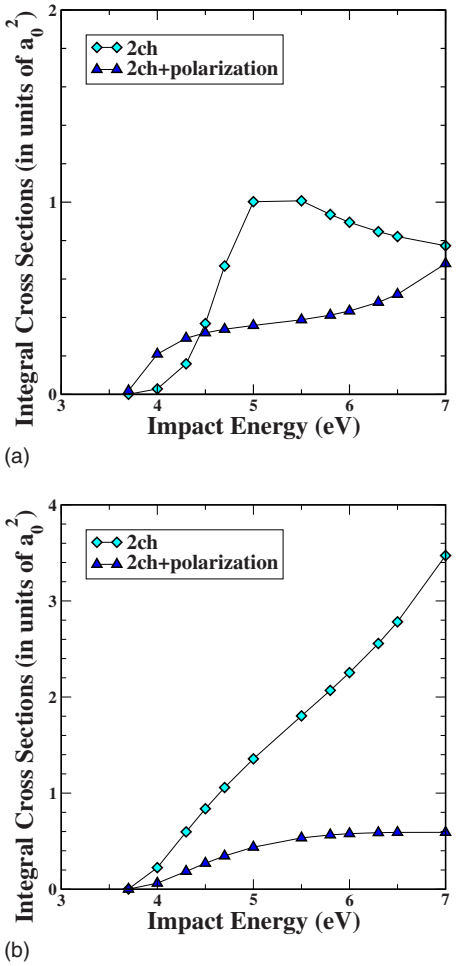

FIG. 2. (Color online) Integral cross sections for the $^1A_1 \rightarrow {}^3B_2$ electronic transition (inelastic) of the furan molecule: (a) $^2A_2$ symmetry and (b) $^2B_1$ symmetry. In the legend box: "2ch" means that elastic ($^1A_1$) and inelastic ($^3B_2$) channels are open.

V. CONCLUSIONS

We employed the SMC method to investigate the influence of polarization effects on the electronic excitation cross section of furan by electron impact. This molecule was considered as an important prototype because it has similarities to more complicated biological molecules. Our study shows that polarization effects can strongly influence electronic excitation cross sections for molecular systems supporting resonances near low-energy thresholds. Simple close-coupling calculations may furnish meaningless results if carried out without a proper treatment of polarization effects, due to the presence of misplaced resonances.

ACKNOWLEDGMENTS

The authors acknowledge financial support from the Brazilian agencies Fundação de Amparo à Pesquisa do Estado de São Paulo (FAPESP) and Conselho Nacional de Desenvolvimento Científico e Tecnológico (CNPq). One of the authors (M.H.F.B.) acknowledges support from the Paraná State agency Fundação Araucária and from Finep. The authors acknowledge computational support from CENAPAD-SP.

[1] B. Boudaïffa, P. Cloutier, D. Hunting, M. A. Huels, and L. Sanche, Science **287**, 1658 (2000); L. Sanche, Eur. Phys. J. D **35**, 367 (2005); F. Martin, P. D. Burrow, Z. Cai, P. Cloutier, D. Hunting, and L. Sanche, Phys. Rev. Lett. **93**, 068101 (2004).
[2] A. Zecca, C. Perazzolli, and M. J. Brunger, J. Phys. B **38**, 2079 (2005).
[3] P. Mozejko and L. Sanche, Radiat. Phys. Chem. **73**, 77 (2005).
[4] C. König, J. Kopyra, I. Bald, and E. Illenberger, Phys. Rev. Lett. **97**, 018105 (2006).
[5] C. Winstead and V. McKoy, J. Chem. Phys. **125**, 244302 (2006).
[6] C. Winstead and V. McKoy, J. Chem. Phys. **125**, 074302 (2006).
[7] D. Bouchiha, J. D. Gorfinkiel, L. G. Caron, and L. Sanche, J. Phys. B **39**, 975 (2006).
[8] C. S. Trevisan, A. E. Orel, and T. N. Rescigno, J. Phys. B **39**, L255 (2006).
[9] C. J. Colyer, V. Vizcaino, J. P. Sullivan, M. J. Brunger, and S. J. Buckman, New J. Phys. **9**, 41 (2007).
[10] M. H. F. Bettega and M. A. P. Lima, J. Chem. Phys. **126**, 194317 (2007).
[11] T. Fleig, S. Knecht, and C. Hättig, J. Phys. Chem. A **111**, 5482 (2007).
[12] A. Modelli and P. W. Burrow, J. Phys. Chem. A **108**, 5721 (2004).
[13] P. Sulzer, S. Ptasinska, F. Zappa, B. Mielewska, A. R. Milosavljevic, P. Scheier, T. D. Märk, I. Bald, S. Gohlke, M. A. Huels, and E. Illenberger, J. Chem. Phys. **125**, 044304 (2006).
[14] M. H. Palmer, I. C. Walker, C. C. Ballard, and M. F. Guest, Chem. Phys. **192**, 111 (1995).
[15] K. Takatsuka and V. McKoy, Phys. Rev. A **30**, 1734 (1984).
[16] M. H. F. Bettega, L. G. Ferreira, and M. A. P. Lima, Phys. Rev. A **47**, 1111 (1993).
[17] R. F. da Costa, F. J. da Paixão, and M. A. P. Lima, J. Phys. B **38**, 4363 (2005).
[18] G. B. Bachelet, D. R. Hamann, and M. Schlüter, Phys. Rev. B **26**, 4199 (1982).
[19] M. H. F. Bettega, A. P. P. Natalense, M. A. P. Lima, and L. G. Ferreira, Int. J. Quantum Chem. **60**, 821 (1996).
[20] P. Chaudhuri, Marcio T. do N. Varella, C. R. C. de Carvalho, and M. A. P. Lima, Phys. Rev. A **69**, 042703 (2004).
[21] W. J. Hunt and W. A. Goddard, Chem. Phys. Lett. **3**, 414 (1969).
[22] J. Wan, J. Meller, M. Hada, M. Ehara, and H. Nakatsujia, J. Chem. Phys. **113**, 7853 (2000).
[23] A. Giuliani and M.-J. Hubin-Franskin, Int. J. Mass Spectrom. **205**, 163 (2001).
[24] M. Allan (private communication).
[25] C. W. Bauschlicher, J. Chem. Phys. **72**, 880 (1980).
[26] C. Winstead, V. McKoy, and M. H. F. Bettega, Phys. Rev. A **72**, 042721 (2005).